

# Open-source implementation of the new unified CPT-based axial method in sands

Carlos Sastre Jurado<sup>1,2\*</sup>, Bruno Stuyts<sup>1,2</sup>

<sup>1</sup> UGent, Geotechnical Laboratory, Technologiepark 68, Zwijnaarde, 9052, Belgium

<sup>2</sup> OWI-Lab, Vrije Universiteit Brussel, Pleinlaan 2, B-1050 Brussels, Belgium

\* Corresponding author: carlos.sastrejurado@ugent.be

## ABSTRACT

This paper presents the implementation into the open-source finite element simulation framework OpenSees of the new Unified CPT-based method for driven piles in sands. The formulation incorporates the maximum skin friction and end-bearing CPT values based on the new ISO-19901-4 under development, within the non-linear load-transfer curves calibrated against the measured responses from the static pile tests in the unified database. Special attention was paid to maintaining an open-source philosophy during the implementation. The important EURIPIDES research tests in highly dense sands are considered as a worked example to illustrate the application of the implemented method. The numerical benchmark shows good agreement between the model and full-scale measurements.

**Keywords:** open-source; cone penetration test (CPT); driven piles; sands.

## 1. Introduction

In the 90s, the static axial capacity of open-ended pipe piles in sand was an area of great uncertainty, and the only globally recognized design method available was provided in the American Petroleum Institute (API) recommendations (1993). This motivated the development of new calculation procedures based on results from several full-scale pile load tests over the following years. As a result, the API Recommended Practice (RP2A) for fixed offshore structures (2006) considered four additional design methodologies for driven piles in sand:

- the Fugro method, referred to as Fugro-05 (Kolk, Baaijens, and Senders 2005);
- the Imperial College London method, referred to as ICP-05 (Jardine et al. 2005);
- the Norwegian Geotechnical Institute method, referred to as NGI-05 (Clausen, Aas, and Karlsrud 2005);
- the University of Western Australia method, referred to as UWA-05 (B. Lehane, J. Schneider, and Xu 2007).

All of these methods are based on the cone resistance profile ( $q_c$ ) measured by the Cone Penetration Test (CPT), and they are outlined in the informative Appendix of the API RP 2GEO (2011) standard. In granular soils, the API

design method, referred to as the  $\beta$ -method, assumes that both ultimate local shaft friction and ultimate unit base resistance are proportional to the vertical effective stress, through the  $\beta$  and  $N_q$  factors. Design guidelines to define values for those factors and for limiting values on shaft friction and end bearing are given as a function of the soil type. For certain soil types like very loose sand, the current API methodology does not provide any guidance, and CPT-based methods may offer a viable alternative that can yield reliable results.

The reliability of the CPT-based methods was assessed against the compiled UWA database of load tests on driven piles in siliceous sands at sites with CPT measurements (Schneider, Xu, and Lehane 2008). Nevertheless, it was concluded that uncertainty still remains in the static pile capacity estimation, and no clear guidance existed about which method should be employed by designers.

To further enhance offshore pile design criteria, a large number of driven pile load tests were reviewed to establish a so-called *Unified Database*, which included 71 conducted tests in sandy locations (Lehane et al. 2017). Subsequently, the four CPT-based methods recommended in the API guidelines were consolidated into a single unified method. This new *Unified* CPT-based axial pile capacity design method was calibrated against the gathered pile load test database (Lehane et al. 2020). Load-transfer curve formulae were also developed and validated against the unified database (Lehane, Li, and Bittar 2020).

This work aims to present the open-source implemen-

tation and validation of the recently developed CPT-based method in sands. Shaft and base load transfer curves were included in the Open Source for Earthquake Engineering Simulation platform (OpenSees) (McKenna 2011). OpenSees promotes innovation in research and advanced applications for practice, thus it has the potential to become a community code for finite element (FE) analysis in geotechnical engineering. Examples of the latter are the implemented commands `PySimple1Gen` and `TzSimple1Gen` for seismic soil-pile-structure interaction analysis (Boulanger et al. 1999; Brandenburg and Boulanger 2022), or the recently proposed SANISAND-MS model (Liu et al. 2022) to support the cyclic analysis of offshore foundations. The important EURIPIDES axial pile load tests (Zuidberg and Vergobbi 1996) in dense sand are considered as a worked example to illustrate the application of the implemented method.

The structure of the paper is as follows. Section 2 briefly describes the unified CPT-based method and its main equations for axial capacity and axial load transfer calculations. The implementation of the shaft and base load transfer curves in OpenSees for the unified method is described in Section 3. Section 4 presents the numerical benchmark against the pile load test results from the EURIPIDES project, and Section 5 summarizes the main conclusions.

## 2. Unified CPT-based method in sands

### 2.1. Axial pile capacity

The static axial bearing capacity of a deep foundation is calculated as the sum of the shaft capacity ( $Q_{\text{shaft}}$ ) and end bearing or base capacity ( $Q_{\text{base}}$ ), which has no contribution for tension loading. The new unified CPT method for sands is described in detail by (Lehane et al. 2020), and the main equations are only briefly introduced here.

#### 2.1.1. Shaft capacity

A Coulomb frictional law is assumed to estimate the local ultimate shaft friction,  $\tau_f$ , as follows:

$$\tau_f = (f_t/f_c) (\sigma'_{rc} + \Delta\sigma'_{rd}) \tan \delta_f \quad (1)$$

where  $\sigma'_{rc}$  is the (stationary) radial effective stress,  $\Delta\sigma'_{rd}$  is the increase in radial effective stress that occurs during pile loading attributed to dilation effects. The term  $\delta_f$  stands for the ultimate sand-pile interface friction angle, which can be obtained by performing drained ring shear interface tests. In the absence of site-specific measurements, a constant value of  $29^\circ$  is recommended. The coefficient  $f_t/f_c$

becomes 1 for compression loading and 0.75 for tension loading due to the Poisson ratio effect.

The term  $\sigma'_{rc}$  is calculated according to Eq. 2:

$$\sigma'_{rc} = (q_c/44) A_{re}^{0.3} [\text{Max}[1, (h/D)]]^{-0.4} \quad (2)$$

where  $h$  refers to the distance from the pile tip to a given soil depth,  $D$  is the outer pile diameter and  $A_{re}$  represents the effective area ratio which is given in Eq. 3. Note that for a closed ended pile  $A_{re}$  becomes 1.

$$A_{re} = 1 - \text{PLR} (D_i/D)^2 \quad (3)$$

being  $D_i$  the pile inner diameter and PLR the so called plug length ratio (ratio of the plug length to the pile embedment). The latter can be approximated by Eq. 4, in which  $d_{CPT}$  is diameter of the standard CPT probe with a nominal value of 35.7mm.

$$\text{PLR} \approx \tanh \left[ 0.3 (D_i/d_{CPT})^{0.5} \right] \quad (4)$$

The  $\Delta\sigma'_{rd}$  term in Eq. 1 can be calculated as follows:

$$\Delta\sigma'_{rd} = \left( \frac{q_c}{10} \right) \left( \frac{q_c}{\sigma'_v} \right)^{-0.33} \left( \frac{d_{CPT}}{D} \right) \quad (5)$$

#### 2.1.2. Base capacity

The expression for the base capacity is:

$$Q_{\text{base}} = q_{b0.1} (\pi D^2/4) \quad (6)$$

where  $q_{b0.1}$  is the ultimate unit base resistance mobilized at a settlement of 10% of the pile diameter, given by Eq. 7.

$$q_{b0.1} = [0.12 + 0.38 A_{re}] q_p \quad (7)$$

The parameter  $q_{b0.1}$  is thus assumed proportional to  $q_p$ , which is the end bearing mobilised at large displacements at the level of the pile base by a pile with a diameter of  $D_{eq} = DA_{re}^{0.5}$ . As discussed in (Lehane et al. 2020), several techniques can be employed for the estimation of  $q_p$ . In sands that are relatively homogeneous, one can consider  $q_p$  to be the average value of  $q_c$  within a zone  $1.5D$  above and below the pile base. In more heterogeneous locations, the equation  $q_p = 1.2q_{c,Dutch}$  (Schmertmann 1978) or the method suggested by (Boulanger and DeJong 2018) may be employed.

## 2.2. Load-transfer functions

Formulation of non-linear axial load-transfer functions as defined by (Lehane, Li, and Bittar 2020) is summarized here. These curves are given in a normalized form as proposed in the API standards. Displacements are normalized

by the pile diameter, and the mobilized friction and end bearing are normalized by the ultimate local shaft friction and end bearing capacity, respectively.

### 2.2.1. Shaft-load transfer function

Shaft-load transfer functions represent the variation of shaft friction with local relative displacement of the pile wall against the soil. They are commonly referred to as  $t$ - $z$  curves, where  $t$  stands for the local friction and  $z$  for the local displacement. This notation will be adopted here, although, to be consistent with the previously presented formulation,  $\tau$  is used to refer to the skin friction.

Several mathematical functions may be used to describe the static non-linear load displacement response (Fellenius 2018). The unified method for sands assumes a parabolic formulae as given in Eq. 8.

$$\frac{\tau}{\tau_f} = \left(\frac{G}{\tau_f}\right) \left(\frac{z}{2D}\right) \left[1 - \frac{z}{2z_f}\right] \quad (8)$$

where the ratio  $G/\tau_f$  is inversely proportional to the displacement  $z_f$  at which the peak shear friction  $\tau_f$  is attained, as shown in Eq.9.

$$\frac{G}{\tau_f} = \frac{4D}{z_f} \quad (9)$$

The API (2011) guidelines recommend a constant value of 0.01 for the normalized peak displacement  $z_f/D$ . The unified method proposes the following expression that allows for a better match with the measured axial backbone curves:

$$\frac{z_f}{D} = \frac{q_c^{0.5} \sigma_v'^{0.25}}{A p_a^{0.75}} \quad (10)$$

where  $p_a$  is the atmospheric pressure, equal to 100 kPa, and  $\sigma_v'$  is the vertical effective stress. The proposed values for  $A$  are 1250 for compression and half of that, i.e., 625, for tension.

### 2.2.2. Base-load transfer function

Unit end bearing,  $q_b$ , is assumed to be fully mobilized at a pile base displacement value of 0.1D in API (2011). This criterion was also maintained in the unified method. The proposed expression to represent the variation of pile base load with base displacement follows a hyperbolic function of the form:

$$\frac{z_b}{D} = 0.01 \left[ \frac{q_b/q_{b0.1}}{1 - 0.9(q_b/q_{b0.1})} \right] \quad (11)$$

with  $z_b$  as the pile base displacement and  $q_{b0.1}$  calculated as indicated in Eq. 7.

## 3. Implementation in OpenSees

The implementation of the CPT-based unified method within the OpenSees framework is summarized here. The axial curves to simulate the load-displacement response of driven piles in sands were included through two new materials in the OpenSees public repository<sup>1</sup>. The soil reaction curves can be set up through the Python interpreter of OpenSees (Zhu, McKenna, and Scott 2018). Documentation<sup>2</sup> was also provided showing how to use the implemented curves.

### 3.1. Shaft-load transfer function

The shaft or skin friction soil curve formulation for sands is implemented in the `TzSandCPT` uniaxial material. The material calculates the maximum skin friction and end-bearing capacities according to the CPT-based formulation previously presented in §2.1. Therefore, the basic soil input parameters are  $q_c$  and  $\sigma_v'$ . Note that to calculate the ultimate shaft friction an estimate of  $\delta_f$  must be assumed (see Eq. 1). The implemented material assumes a default value of 29° as recommended by (Lehane et al. 2020), although the user can input another value in degrees. The input parameters which are related to the pile geometry, are the outer diameter  $D$  and the wall thickness  $t_w$  (rather than the pile internal diameter). The rest of the inputs are related to the methodology, which are  $h$ , the discretization depth step interval  $\Delta z$ ,  $d_{CPT}$  and  $p_a$ .

The correctness of the coded material has been carefully verified. A validation example based on a typical sand site in the Gulf of Mexico, named *Site A* in (B. M. Lehane, J. A. Schneider, and Xu 2005), is presented here and within the documentation. A single soil spring was created to simulate the load-displacement response at 20m depth assuming a pile tip placed at 60 m depth. The assumed inputs are for this example are as follow. The assumed soil inputs are a  $q_c = 39928$  kPa and  $\sigma_v' = 203.8$  kPa. Pile geometry parameters are  $D = 2.44$  m and  $t_w = 44.5$  mm. A distance from the pile tip  $h$  equals to 40 m and  $\Delta z$  of 1 m are retained for demonstration purposes.

The simulated behavior for this example is shown in Figure 1. The backbone curve shows the expected behavior, with a tension capacity equal to 75% as established in the methodology (Lehane et al. 2020). The computed capacities were validated against the spreadsheet program *Axial Capacity Calculator* from the University of Western

1. <https://github.com/OpenSees/OpenSees>

2. <https://github.com/OpenSees/OpenSeesDocumentation>

Australia (UWA calculator), referred to as  $Q_s$  in Figure 1. The peak displacements  $z_f$ , in both tension and compression, were also validated analytically, leading to half of the peak settlement compared to the peak displacement in tension.

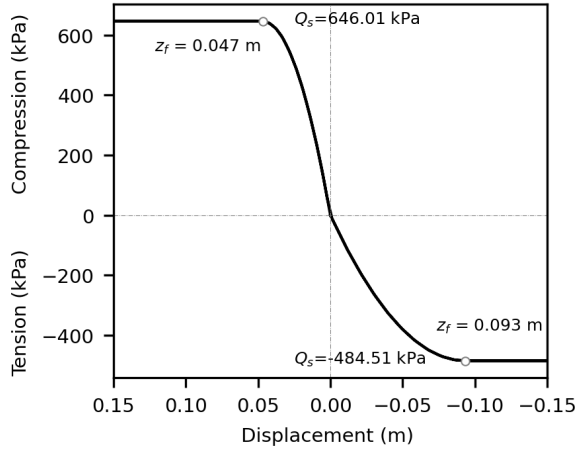


**Figure 1.** Validation example of simulated shaft displacement curve through the implemented TzSandCPT material in OpenSees.

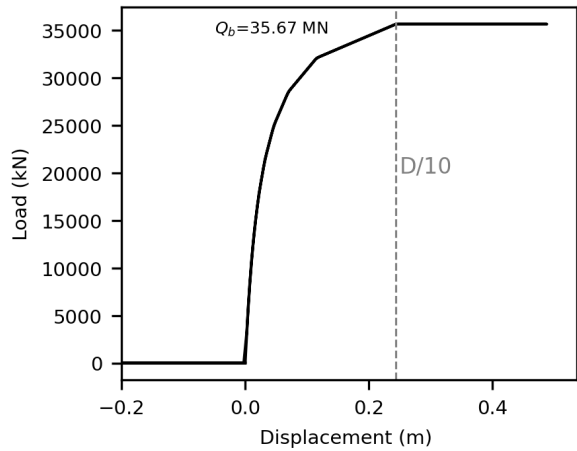


**Figure 2.** Validation example of simulated end bearing displacement curve through the implemented QbSandCPT material in OpenSees.

### 3.2. Base-load transfer function

The QbSandCPT function implements the base-load transfer function, commonly referred to as the  $q - z$  curve. The non-linear end bearing-displacement response obeys

the hyperbolic function. The soil inputs are  $q_c$  and  $\sigma'_v$ , and the pile inputs are  $D$  and  $t_w$ .

An example of the simulated behavior is shown in Figure 2. The same input data as for the shaft curve in § 3.1 was retained also for illustration purposes. As expected, for tension loading, there is no end bearing. The ultimate base capacity is achieved for a settlement of  $0.1D$  as defined in the formulation. The computed base capacity matches the calculated value by (UWA calculator) of 35.67 MN, corresponding to a  $q_{b0.1}$  value of 7.629MN.

## 4. Benchmark against EURIPIDES

The unified database (Lehane et al. 2017) considers the pile tests performed within the framework of the EURIPIDES joint industry project (JIP). The testing program at the EURIPIDES site comprised a series of tension, compression, and cyclic load tests conducted at two specific locations. These tests are part of the unified sand database and were used to calibrate the unified CPT-based method.

A comparison between numerical predictions using the implemented unified CPT method through OpenSees and measurements from the EURIPIDES project is presented here. The comparison against the full-scale measurements has thus a dual purpose. On one hand, it aims to further verify the correctness of the implementation, and on the other hand, it presents a detailed and comprehensive benchmark that also demonstrates the modeling capabilities and facilities.

### 4.1. Site and test pile

The test site is located at Eemshaven, The Netherlands. The encountered soil profile consists of Holocene sands in the first 16 m depth, followed by alternating layers of soft clay and loose sandy silt up to 22 m depth. The overconsolidated stratum of interest for the pile load test is located below 22 m below the ground level, formed by dense to very dense Pleistocene sands with  $q_c$  values in the order 40 MPa to 80 MPa. The average depth of the water table was about 2.0 m. The CPT profile and soil stratigraphy at the second tested location, which will be the focus for comparison purposes in this work, are shown in Figure 3.

The test pile was made of E460N steel and had an external diameter of 0.76 m. The lower segment, extending to a depth of 27 m, was extensively equipped and with a wall thickness of 36 mm. The instrumentation in this lower section aimed to analyze soil-pile interaction along the dense sands below 22 m depth. The upper add-on section had no instrumentation except near the pile head and had a wall thickness of 42 mm. On the lower part of the test pile, fourteen levels of axial strain gauges were installed to gauge

the distribution of axial forces and calculate static shaft resistances. These axial strain gauges were placed at 0.5D, 1.0D, 2.0D, 4.0D, 6.0D, and 8.0D above the pile toe, with additional measurements every 4.0D up to the highest level at approximately 40D. A detailed description of load testing and instrumentation can be found in (Zuidberg and Vergobbi 1996).

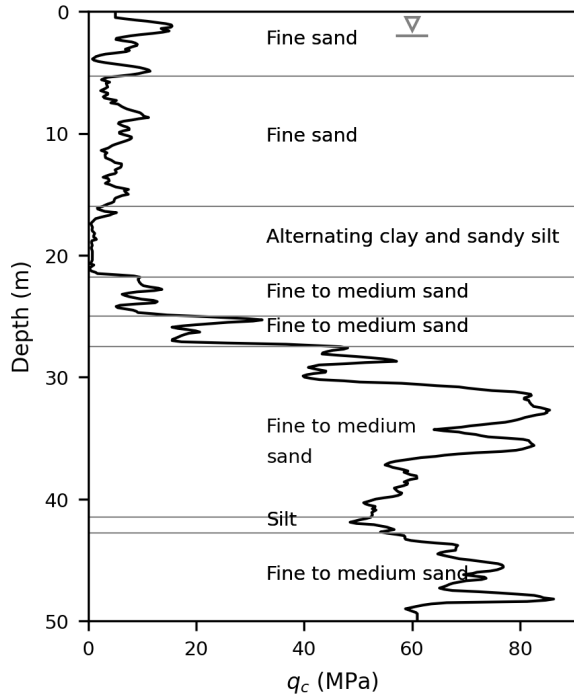


**Figure 3.** CPT41 cone resistance profile and stratigraphy from BH42 at Location II, adapted from (Kolk, Baaijens, and Vergobbi 2005).

#### 4.2. Finite element analyses

The finite element (FE) analysis is based on the implemented load-transfer functions ( $t - z$  and  $q - z$  elements) acting at a series of pile elements. The pile structure was modeled through elastic shear beams, resulting in a total of 467 force-based elements (with a space between nodes equal to 0.1 m). It's worth to note that despite the relatively high number of elements the computation time remains limited, and the analysis is completed in a matter of seconds. The mechanical properties assumed for the pile steel are a Young's modulus of 210 GPa and a Poisson's ratio of 0.3.

According to the recommendations in (B. M. Lehane, J. A. Schneider, and Xu 2005), a spacing of 0.1 m was retained to discretize the  $q_c$  profile from the CPT41 test

(see Figure 3). The averaging approach along a distance of  $1.5D$  above and below the pile tip was used to estimate  $q_p$ , resulting in a value of about 73 MPa. The vertical overburden effective stress profile was inferred from the unit weight estimates reported for each layer (Jardine et al. 2005), assuming a water table level at 2 m depth.

The pile tests were simulated using a displacement-controlled static analysis with a constant axial displacement increment of 1 mm. To solve the non-linear equations, the Newton-Raphson algorithm is employed. The interested reader can further check how the employed FE modeling framework can be used in practice. For this, a tutorial based on the EURIPIDES worked example from (Jardine et al. 2005) is provided in the OpenSees documentation.

#### 4.3. Results

The test results interpreted and reported by (Kolk, Baaijens, and Vergobbi 2005) at the second location and at a penetration depth of 46.7 m (II-46.7) are compared against the simulations. After the nomenclature in the unified database, those correspond to the site *EURIPIDES II* and open-ended piles in compression *OET* and in tension *OEC* for the test type. The static loading sequence at Location II was C-T-R-C, where C refers to the compression test, T to the tension test, and R to the reloading test. The first tests in compression and tension, prior to the reloading operation to bring back the pile to the virgin position, were analyzed here.

The comparison of the compression load-displacement curve derived at the pile head level is shown in Figure 4.

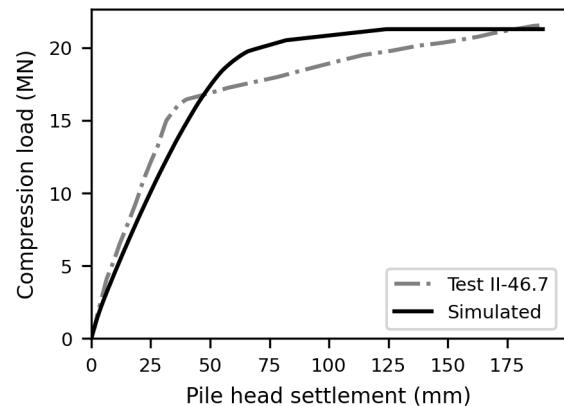


**Figure 4.** EURIPIDES II OEC: Simulated and measured load-displacement response in compression at the pile head.

As expected from (Lehane et al. 2020; Lehane, Li, and Bittar 2020), test and numerical results are in good agree-

ment since the unified method was calibrated against the EURIPIDES tests from the unified database. Nevertheless, full-scale measurements seem to show a stiffer behavior and then a strain-hardening response. This latter effect cannot be captured by the employed methodology since, by definition, it considers a plastic resistance. In this regard, the computed total capacity from the presented FE analysis is 21.2 MN. This estimate is very close to the predicted total capacity of 20.9 MN by other researchers (Wen et al. 2023) assuming the CPT unified method.

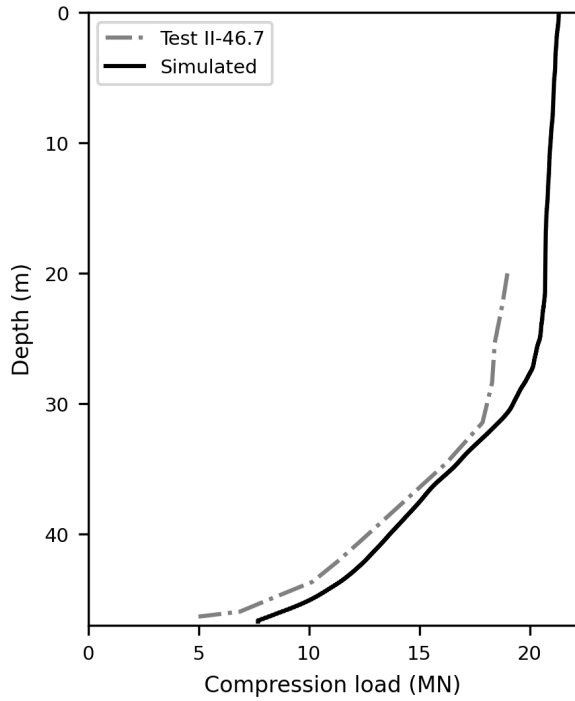


**Figure 5.** EURIPIDES II OEC: Simulated and measured pile axial load distribution for 0.1D base displacement in compression.

The axial load distribution inferred from the installed strain gauges along the embedded pile length for a pile toe displacement around  $0.1D$  (76 mm) was also reported by (Kolk, Baaijens, and Vergobbi 2005). Axial forces along the embedded pile length were also computed through the pile response analysis (t-z and q-z curves) which allows estimation of the load transfer to the soil. Numerical and test results at  $0.1D$  pile toe displacement are presented in Figure 5, showing similar trends, although some deviations are observed. The FE predicts a greater shaft load above 30 m. This mismatch is consistent with results from Figure 4; the model calculates a softer response for the analyzed displacement. Below 30 m, along the very dense sands layer, a better agreement is observed, although the model suggests further mobilization of the pile tip resistance. On the other

hand, the latter comparison might be less reliable, as explained by (Kolk, Baaijens, and Vergobbi 2005), since the measurement uncertainty increases nearer the pile base.

The results from the tension test simulations are presented below.

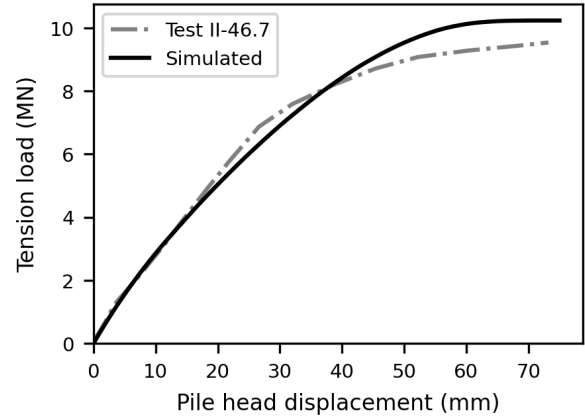


**Figure 6.** EURIPIDES II OET: Simulated and measured load-displacement response in tension at the pile head.

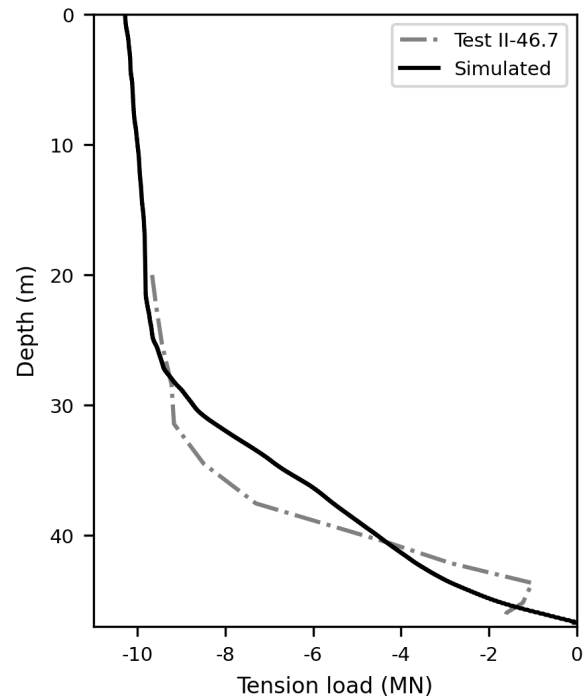


**Figure 7.** EURIPIDES II OET: Simulated and measured pile axial load distribution for 0.1D base displacement in tension.

Similarly, the axial force comparison at the pile head is depicted in Figure 6. It can be seen that the simulated curve

matches remarkably well with the measured axial load for displacements lower than 40 mm. The computed axial resistance under tension loading is 10.2 MN.

Figure 7 presents the same analysis as Figure 5 but under tension loading. Measurements and simulations present a close fit between 20 and 27 m depth. Greater deviations are found when comparing the shaft load distribution along the following very dense sand layer up to 40 m depth. Then, as theoretically expected, the simulated axial load tends to zero when approaching the pile toe, as no end-bearing resistance should be mobilized in tension. This is not observed in the measurements, presumably due to the poor data quality from the strain gauges close to the pile toe.

## 5. Conclusions

This contribution presents the implementation and validation of the unified CPT-based method for the axial behavior of driven piles in sands (Lehane et al. 2020) through the OpenSees FE platform. The modeling capabilities are demonstrated by simulating the well-known EURIPIDES tests, showing good agreement between numerical and experimental results. Special attention was paid to maintaining an open-source philosophy during the implementation, providing documentation and tutorial worked examples in the repository. While the files are being published in the official repository, they have been made publicly accessible in a separate repository<sup>3</sup>. This implementation allows simulation of pile behavior based on the load-transfer functions calibrated against the unified sand database (Lehane, Li, and Bittar 2020). This enables both pile capacity and settlement calculation.

## Acknowledgements

The authors would like to thank the Belgian Ministry of Economic Affairs for their support with the ETF project WINDSOIL. VLAIO's assistance through the De Blauwe Cluster SBO SOILTWIN project is also recognized.

## References

- Boulanger, R. W., C. J. Curras, B. L. Kutter, D. W. Wilson, and A. Abghari. 1999. "Seismic soil-pile-structure interaction experiments and analyses." *J Geotech Geoenviron Eng* 125 (9): 750–759. [https://doi.org/10.1061/\(ASCE\)1090-0241\(1999\)125:9\(750\)](https://doi.org/10.1061/(ASCE)1090-0241(1999)125:9(750)).
- Boulanger, R. W., and J. T. DeJong. 2018. "Inverse filtering procedure to correct cone penetration data for thin-layer and transition effects." In *Proc., Cone Penetration Testing*, 25–44. Delft Univ. of Tech., The Netherlands.
- Brandenberg, S. J., and R. W. Boulanger. 2022. "OpenSees Beam on Nonlinear Winkler Foundation Modeling of Pile Groups in Liquefied and Laterally Spreading Ground in Centrifuge Tests.," <https://escholarship.org/uc/item/6z40d9td>.
- Clausen, CJF, PM Aas, and K Karlsrud. 2005. "Bearing capacity of driven piles in sand, the NGI approach." In *Proceedings of Proceedings of International Symposium. on Frontiers in Offshore Geotechnics, Perth*, 574–580.
- Fellenius, B. H. 2018. "Discussion of "development of axial pile load transfer curves based on instrumented load tests" by cécilia bohn, alexandre lopes dos santos, and roger frank." *J Geotech Geoenviron Eng* 144 (4): 07018005. [https://doi.org/https://doi.org/10.1061/\(ASCE\)GT.1943-5606.0001867](https://doi.org/https://doi.org/10.1061/(ASCE)GT.1943-5606.0001867).
- Jardine, R. J., F. Chow, R. Overy, and J. Standing. 2005. *ICP design methods for driven piles in sands and clays*. Thomas Telford Publishing. <https://doi.org/10.1680/idmfdpisac.32729>.
- Kolk, H. J., A. E. Baaijens, and M. Senders. 2005. "Design criteria for pipe piles in silica sands." In *Design criteria for pipe piles in silica sands*, 711–716. CRC Press/Balkema.
- Kolk, H. J., A. E. Baaijens, and P. Vergobbi. 2005. "Results of axial load tests on pipe piles in very dense sands: The EURIPIDES JIP." In *Frontiers in Offshore Geotechnics: ISFOG*, 661–667.
- Lehane, B., J. Schneider, and X. Xu. 2007. "Development of the UWA-05 Design Method for Open and Closed Ended Driven Piles in Siliceous Sand," 1–10. October. ISBN: 978-0-7844-0902-2. [https://doi.org/10.1061/40902\(221\)12](https://doi.org/10.1061/40902(221)12).
- Lehane, B. M., L. Li, and E. J. Bittar. 2020. "Cone penetration test-based load-transfer formulations for driven piles in sand." *Geotech Lett* 10 (4): 568–574. <https://doi.org/https://doi.org/10.1680/jgele.20.00096>.

---

3. [https://csasj.github.io/FEM\\_OpenSees/](https://csasj.github.io/FEM_OpenSees/)

- Lehane, B. M., J. K. Lim, P. Carotenuto, F. Nadim, S. Lacasse, R. J. Jardine, and B. F. J. Van Dijk. 2017. "Characteristics of unified databases for driven piles." In *Proceedings of the 8th International Conference of Offshore Site Investigation and Geotechnics OSIG, London, UK*, 12–14.
- Lehane, B. M., J. A. Schneider, and X. Xu. 2005. *A Review of Design Methods for Offshore Driven Piles in Siliceous Sand*. September.
- Lehane, B. M., L. Zhongqiang, E. J. Bittar, F. Nadim, S. Lacasse, R. J. Jardine, P. Carotenuto, M. Rattley, and K. Gavin. 2020. "A New 'Unified' CPT-Based Axial Pile Capacity Design Method for Driven Piles in Sand" [in English]. In *Proceedings Fourth International Symposium on Frontiers in Offshore Geotechnics*, edited by Zack Westgate, 462–477. <https://www.isfog2020.org/>.
- Liu, H., E. Kementzetzidis, J. A. Abell, and F. Pisanò. 2022. "From cyclic sand ratcheting to tilt accumulation of offshore monopiles: 3D FE modelling using SANISAND-MS." *Geotech* 72 (9): 753–768. <https://doi.org/10.1680/jgeot.20.P.029>.
- McKenna, F. 2011. "OpenSees: a framework for earthquake engineering simulation." *Comput. Sci. Eng.* 13 (4): 58–66. <https://doi.org/10.1109/MCSE.2011.66>.
- Schmertmann, J. H. 1978. *Guidelines for cone penetration test : performance and design*. United States. Federal Highway Administration. Office of Research / Development. <https://rosap.nrl.bts.gov/view/dot/958>.
- Schneider, J. A., X. Xu, and B. M. Lehane. 2008. "Database assessment of CPT-based design methods for axial capacity of driven piles in siliceous sands." *J Geotech Geoenviron Eng* 134 (9): 1227–1244. [https://doi.org/https://doi.org/10.1061/\(ASCE\)1090-0241\(2008\)134:9\(1227\)](https://doi.org/https://doi.org/10.1061/(ASCE)1090-0241(2008)134:9(1227)).
- UWA calculator. *Axial Capacity Calculator using CPT*. <https://pile-capacity-uwa.com/>.
- Wen, Kai, Stavroula Kontoe, Richard J Jardine, Tingfa Liu, David Cathie, Rui Silvano, Chiara Prearo, Shipeng Wei, Felix C Schroeder, and Stanislas Po. 2023. "Assessment of time effects on capacities of large-scale piles driven in dense sands." *Canadian Geotechnical Journal*.
- Zhu, M., F. McKenna, and M. H. Scott. 2018. "OpenSeesPy: Python library for the OpenSees finite element framework." *SoftwareX* 7:6–11. <https://doi.org/https://doi.org/10.1016/j.softx.2017.10.009>.
- Zuidberg, H. M., and P. Vergobbi. 1996. "EURIPIDES, load tests on large driven piles in dense silica sands." In *Offshore Technology Conference, OTC-7977*. OTC.